Parallel Pumping of Europium and Yttrium Iron Garnets at Low Temperatures

W. G. NILSEN, R. L. COMSTOCK,* AND L. R. WALKER
Bell Telephone Laboratories, Murray Hill, New Jersey
(Received 17 February 1965)

The spin-wave dispersion and relaxation properties as well as magnetoelastic and elastic properties of europium iron garnet (EuIG) and yttrium iron garnet (YIG) are measured at low temperatures and at about 17 Gc/sec using the parallel-pump technique. Eu^{3+} ions have unusual magnetic and relaxation characteristics in large exchange fields, and the effect of these ions on the spin-wave spectrum of the iron lattice is of interest. Also, the large effective magnetoelastic coupling constant of EuIG along [111] should have a marked effect on the character of the threshold curve as well as the magnon-phonon interaction notch. We find that the spin-wave linewidth of YIG is less than that of EuIG and that the three-magnon confluence process does not account quantitatively for the k-dependent linewidth at low temperatures. The exchange constant of EuIG is predicted quite well from the known magnetic properties of the Eu^{3+} ion and its expected effect on the spin-wave spectrum of the iron lattice. The large magnetoelastic coupling constant of EuIG along [111] makes the threshold curve quite anomalous. It shifts the longitudinal notch to higher k values, yielding an erroneously high exchange constant. Also, the shear-wave notch is absent, possibly because the spin-wave instability merges smoothly into the elastic-wave instability. Along [100], the coupling constant of EuIG is much smaller and a normal threshold curve is obtained. For YIG, the magnetoelastic coupling constants derived from parallel-pump measurements are significantly higher than those obtained from strain-gauge measurements. This might be due to the lower temperature at which the parallel-pump measurements were done. For EuIG, the agreement between the two kinds of measurements was reasonably good. The elastic Q increases with decreasing temperature for both garnets and is larger for YIG than for EuIG, as expected.

INTRODUCTION

THE narrow magnetic-resonance linewidth found[1] for europium iron garnet (EuIG) at low temperatures made it appear possible to do parallel-pumping[2,3] experiments on this material at reasonable power levels. Our interest in such experiments was to measure some of the magnetic and elastic properties of EuIG at high frequencies and to compare these properties of EuIG with those of yttrium iron garnet (YIG). In parallel-pumping experiments, spin waves with well-defined wave vectors (**k**) are excited by applying an rf magnetic field of sufficient intensity parallel to the dc magnetic field. The experimental results are usually summarized by a threshold curve which shows the rf field intensity required to initiate the spin-wave instability as a function of the k value of the excited spin wave. Such experiments yield considerable information about the magnetic and elastic properties of a ferromagnetic insulator. For example, the relaxation characteristics of spin waves can be studied as a function of the wave vector since **k** varies with dc magnetic field intensity. Also, spin waves can couple to shear and longitudinal elastic waves of the same frequency and wave vector.[2,4] This coupling causes, at certain dc magnetic fields, a sudden increase in the rf field intensity required to initiate instability. Since the wave number of the elastic wave can be found from its velocity, these notches in the threshold curve serve to identify the wave number of the spin waves excited at certain dc fields from which the exchange constant in the dispersion relation for spin waves can be determined.[5,6] The height and width of the notch also yield information about the magnetoelastic coupling constant and about the elastic losses in the sample.[6] Such measurements have been reported for yttrium iron garnet by Olson[7] down to 77°K and for lithium ferrite by Comstock and Nilsen[8] at room temperature.

The present paper reports some parallel pumping experiments on EuIG and YIG at 4.2 and 20.4°K. At these low temperatures the magnetic-resonance linewidth of EuIG is quite small (less than 1 Oe) since the relaxation effects of the $J=0$ ground state of Eu^{3+} are small and the $J=1$ state essentially is not occupied. Also, this ground state exhibits only an induced magnetic moment originating from the off-diagonal elements of the magnetic-moment matrix. This induced magnetic moment is coupled antiferromagnetically to the tetrahedral ions in the iron lattice so that the total magnetic moment of EuIG is less than that of YIG.[9] Indeed, part of our interest in comparing EuIG and YIG is to determine the effect of an ion with an induced moment in the rare-earth site on the magnetic and relaxation characteristics of the iron lattice. In addition, EuIG has a very large magnetoelastic coupling constant along [111], and its effect on the interaction between spin waves and elastic waves is of interest.

---

* Present address: Lockheed Research Laboratories, Palo Alto, California.

[1] R. C. LeCraw, W. G. Nilsen, J. P. Remeika, and J. H. Van Vleck, Phys. Rev. Letters **11**, 532 (1963).

[2] E. Schlömann, Raytheon Company, Research Division, Technical Report No. R-48, 1959 (unpublished) E. Schlömann, J. J. Green, and U. Milano, J. Appl. Phys. **31**, 386S (1960).

[3] F. R. Morgenthaler, J. Appl. Phys. **31**, 95S (1960).

[4] E. H. Turner, Phys. Rev. Letters **5**, 100 (1960).

[5] R. C. LeCraw and L. R. Walker, J. Appl. Phys. **32**, 167S (1961).

[6] F. R. Morgenthaler, J. Appl. Phys. **34**, 1289 (1963) [Part 2).

[7] F. A. Olson, J. Appl. Phys. **34**, 1281 (1963) [Part 2].

[8] R. L. Comstock and W. G. Nilsen, Phys. Rev. **136**, A442 (1964).

[9] W. P. Wolf and J. H. Van Vleck, Phys. Rev. **118**, 1490 (1960).

EXPERIMENTAL PROCEDURE

The experiments were done in the way described in an earlier paper by Comstock and Nilsen[8] on the parallel pumping of lithium ferrite. The EuIG was taken from the same batch as the pure sample used in the ferromagnetic linewidth measurements reported in Ref. 1. The YIG was similar in purity to that used by LeCraw and Spencer[10] to study the relaxation of the uniform precession. The polished spheres were about 1 mm in diameter and, for the experiments along the [111] axis, were supported loosely by a Teflon holder at the center of a full wavelength reflection cavity. The spheres were free to rotate and align themselves with the easy [111] axis along the dc magnetic field. Besides ease in aligning samples, the [111] orientation has two advantages over the [100] orientation provided the magnetoelastic coupling constant is not too large. First, the spin waves can couple to longitudinal elastic waves as well as to shear waves,[8] which makes it possible to determine k at one additional magnetic field intensity. Second, the effective magnetoelastic coupling constant along [111] involves both B_1 and B_2 in different combinations for the shear and longitudinal notches so that both B's can be determined from the same threshold curve.

For EuIG, the coupling constant B_1 is very large[11] which makes the threshold curve taken along [111] quite anomalous (Figs. 3 and 4). For this reason, a threshold curve was also measured on EuIG along [100] where the effective magnetoelastic coupling involves only B_2 and is much smaller. A more normal threshold curve was obtained in this case (see Fig. 5). For this experiment, the sphere was aligned and mounted in the cavity so that both dc and rf magnetic fields were along the [100] direction of the garnet. A high pump frequency ($\omega_p \approx 34.7$ Gc/sec) was used so that the sample remained magnetically saturated over the dc fields (and, therefore, k values) of interest. At the same time, the high pump frequency used ensures that the longitudinal- and shear-wave notches are well separated from each other and from the minimum of the threshold curve. The rf magnetic susceptibility of the parallel-pump instability was considerably less for EuIG, but relaxation oscillations were easily observed in the instability regions. In order to obtain high rf-field amplitudes without heating the sample, short ($\sim$100 μsec) microwave pulses were employed with low repetition rates ($\sim$30 pulses/sec). The reflected pulses were monitored on a wide-bandwidth oscilloscope on which the susceptibility and relaxation oscillations were observed.

EXPERIMENTAL RESULTS

The threshold rf magnetic field for spin-wave instability in parallel-pump experiments is given by[2]

$$h_{\rm crit}=\frac{\omega_p}{\omega_m}\left(\frac{\Delta H_{\rm k}}{\sin^2\theta_{\rm k}}\right)_{\rm min}, \tag{1}$$

where ω_p, the pump frequency, is equal to twice the spin-wave frequency, $\Delta H_{\rm k}$ the linewidth of the spin wave being pumped, and $\theta_{\rm k}$ the angle between $\mathbf{k}$ and the static magnetic field ($\mathbf{H}$). The quantity ω_m is defined below. The dispersion relation for spin waves is derived for EuIG in Appendix A and is given by

$$\left(\frac{\omega_p}{2\gamma_{\rm Fe}}\right)^2=\left\{H_i\left(1+\frac{\mathbf{M}_{20}}{\mathbf{M}_{10}}\right)+\left(\mu\mathbf{M}_{10}+2\beta\mathbf{M}_{20}\right)(\mathbf{k}\cdot\mathbf{k})\right\}$$
$$\times\left\{H_i\left(1+\frac{\mathbf{M}_{20}}{\mathbf{M}_{10}}\right)+\left(\mu\mathbf{M}_{10}+2\beta\mathbf{M}_{20}\right)(\mathbf{k}\cdot\mathbf{k})\right.$$
$$\left.+4\pi(\sin^2\theta_k)\left[\frac{(\mathbf{M}_{10}+\mathbf{M}_{20})^2}{\mathbf{M}_{10}}\right]\right\}, \tag{2}$$

where H_i, the internal magnetic field, includes the shape demagnetizing field and the anisotropy field, and $\mathbf{M}_{20}/\mathbf{M}_{10}\equiv(M_{20}/M_{10})\,\mathrm{sgn}\mathbf{M}_{20}\cdot\mathbf{M}_{10}$. The quantities μ and β are calculable constants which depend on the relative locations of the iron ions for μ and iron and europium ions for β. The gyromagnetic ratio of the iron sublattices is denoted by $\gamma_{\rm Fe}$. The resultant magnetic moment $\mathbf{M}$ is given by $(\mathbf{M}_{10}+\mathbf{M}_{20})$, where $\mathbf{M}_{10}$ is the resultant dc magnetic moment of the iron sublattices and $\mathbf{M}_{20}$ is the total dc magnetic moment of the Eu^{3+} ions which is opposite in sign to $\mathbf{M}_{10}$. For YIG, $\mathbf{M}_{20}$ is zero so that in this case Eq. (2) reduces to the ordinary spin-wave dispersion relation.[2]

As can be seen from Eq. (2), the Eu^{3+} ions have two effects on the spin-wave dispersion of the iron lattice. First, the effective magnetic field is reduced by a factor of $(1+\mathbf{M}_{20}/\mathbf{M}_{10})$. Second, the intrinsic exchange constant $D=\mu\mathbf{M}_{10}+2\beta\mathbf{M}_{20}$ is increased by a factor of $(1+2\beta\mathbf{M}_{20}/\mu\mathbf{M}_{10})$. For convenience in writing subsequent equations, we define an effective gyromagnetic ratio $\gamma_{\rm eff}=\gamma_{\rm Fe}(1+\mathbf{M}_{20}/\mathbf{M}_{10})$ and an effective exchange constant $D_{\rm eff}=D/(1+\mathbf{M}_{20}/\mathbf{M}_{10})$. With these definitions, Eq. (2) can be written in the form

$$(\omega_p/2\gamma_{\rm eff})^2=(H_i+D_{\rm eff}k^2)(H_i+D_{\rm eff}k^2+4\pi M\sin^2\theta_k), \tag{3}$$

which more closely resembles the conventional[2] dispersion relation for spin waves. The quantity ω_m used in Eq. (1) is equal to $\gamma_{\rm eff}4\pi M$.

Figures 1–5 show, for EuIG and YIG at 4.2 and 20.4°K, a graph of the instability threshold normalized to the minimum threshold at k near zero, as a function of $|H_c-H|^{1/2}$. Here, H_c is the applied magnetic field for minimum threshold. For static magnetic fields small enough so that $k>0$ ($H<H_c$ in Figs. 1–5), Eq. (1) shows that the excited spin waves propagate at right angles to $\mathbf{H}(\theta_k=\pi/2)$. The relation between wave number and dc magnetic field for spin waves is from Eq. (3):

$$k=[(H_c-H)/D_{\rm eff}]^{1/2} \tag{4}$$

[10] R. C. LeCraw and E. G. Spencer, J. Phys. Soc. Japan **17**, Suppl. B-1, 401 (1962).
[11] S. Iida, Phys. Letters **6**, 165 (1963).

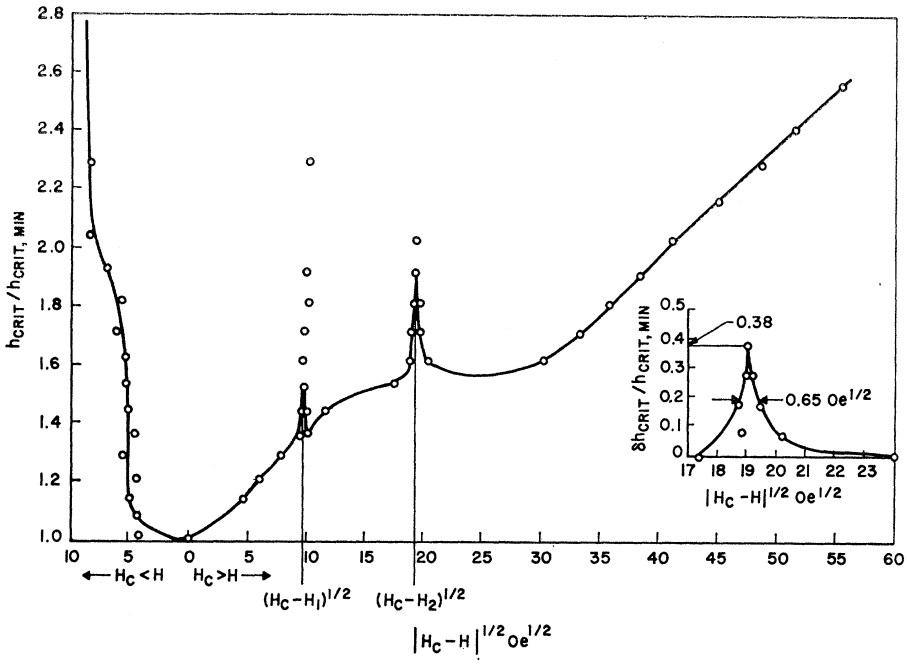

FIG. 1. The parallel-pump threshold curve with **H** parallel to [111] for YIG at 4.2°K normalized to minimum threshold, $h_{crit,min}=0.075$ Oe, at k near zero. For $H<H_c$, the abscissa $|H_c-H|^{1/2}$ is proportional to the k value of excited spin wave. The notches arise from the interaction of spin waves with longitudinal (H_1) and shear (H_2) elastic waves. The single points above the notches indicated pauses or hesitations in the relaxation oscillations, but the curve separates the region of no power absorption from the region where power is absorbed. The inset is an expanded plot of the shear-wave notch. The height and width of the longitudinal-wave notch are 0.17 and 0.31 Oe$^{1/2}$, respectively.

so that in the region $H<H_c$, k varies linearly with $|H_c-H|^{1/2}$. Table I shows a comparison of H_c calculated from known characteristics of EuIG and YIG and H_c determined experimentally in the present work. The good agreement between theory and experiment for YIG tends to support the assumption that the minimum threshold corresponds to k values near zero. The difference between experimental and calculated values of H_c for EuIG is probably due to errors in $H_a{}^e$ and γ_{eff} which were determined[1] at about 11 Gc/sec rather than 17 Gc/sec.

The notches in the threshold curves at dc magnetic

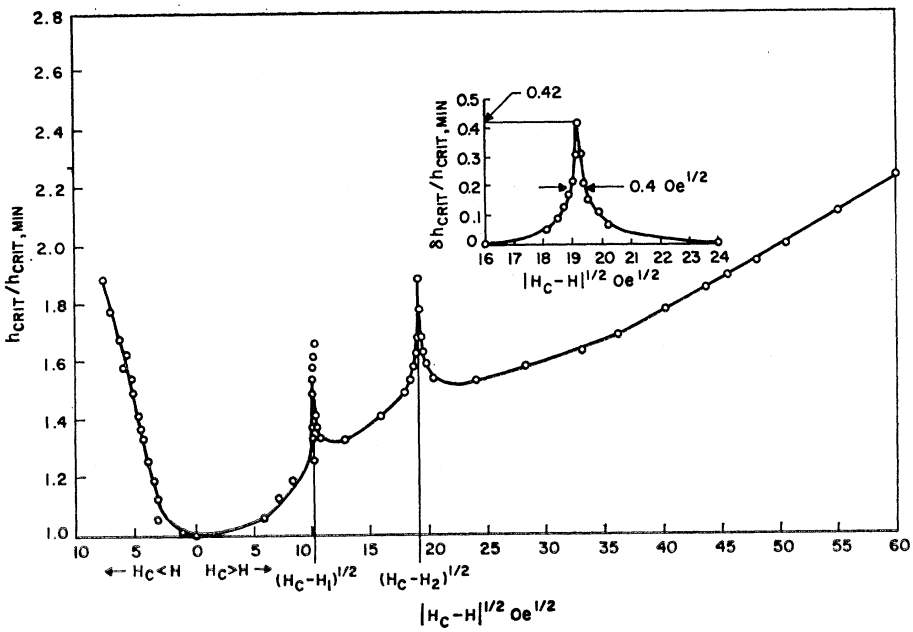

FIG. 2. The parallel-pump threshold curve for YIG at 20.4°K, with **H** along [111]. The minimum threshold $h_{crit,min}$ is 0.31 Oe. The height and width of the longitudinal-wave notch are 0.24 and 0.17 Oe$^{1/2}$, respectively.

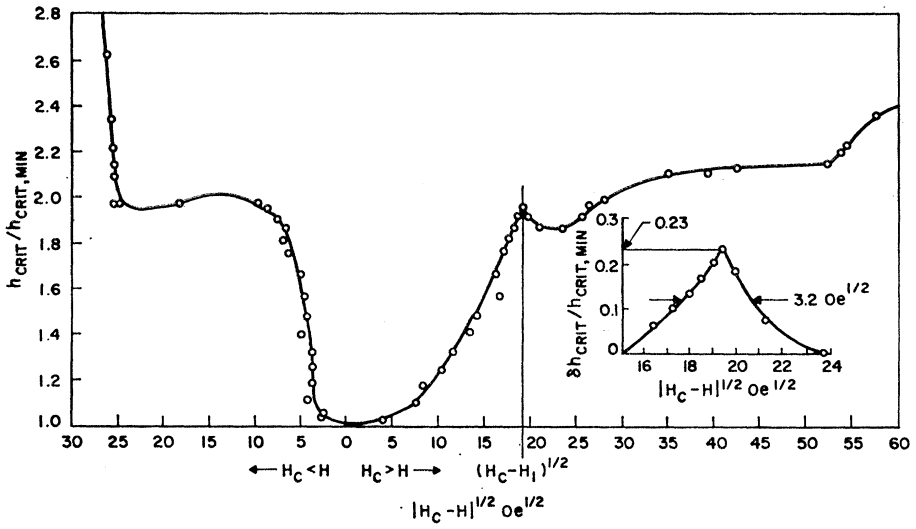

FIG. 3. The parallel-pump threshold curve for EuIG at 4.2°K, with **H** along [111]. The minimum threshold $h_{crit,min}$ is 1.3 Oe.

fields H_1 and H_2 correspond to interactions between spin waves and the longitudinal and transverse elastic waves, respectively. From Eq. (4) and the dispersion relation for the elastic waves, we know that

$$[(H_c-H_2)/(H_c-H_1)]^{1/2}=v_l/v_s, \quad (5)$$

where v_l and v_s are the longitudinal and shear velocities, respectively. This relation is well satisfied both in YIG parallel pumped along [111] at 4.2 and 20.4°K (Figs. 1 and 2) and in EuIG pumped along [100] (Fig. 5) and serves to identify the notches as well as give some confidence in the exchange constants derived from them. The presence of the small longitudinal notch with the magnetic field along [100] (Fig. 5) is probably due to imperfect alignment of the sphere and the large value of B_1. The insets in Figs. 1–5 are expanded plots of the shear- or longitudinal-wave notch. They show the height and width of the notch which are used in finding the elastic Q and magnetoelastic coupling constants. The region on the right of the shear-wave notch in Figs. 1, 2, and 5 ($H<H_2$) corresponds to excitation of nearly pure spin waves of increasing k values. However, for EuIG parallel pumped along the easy axis of magneti-

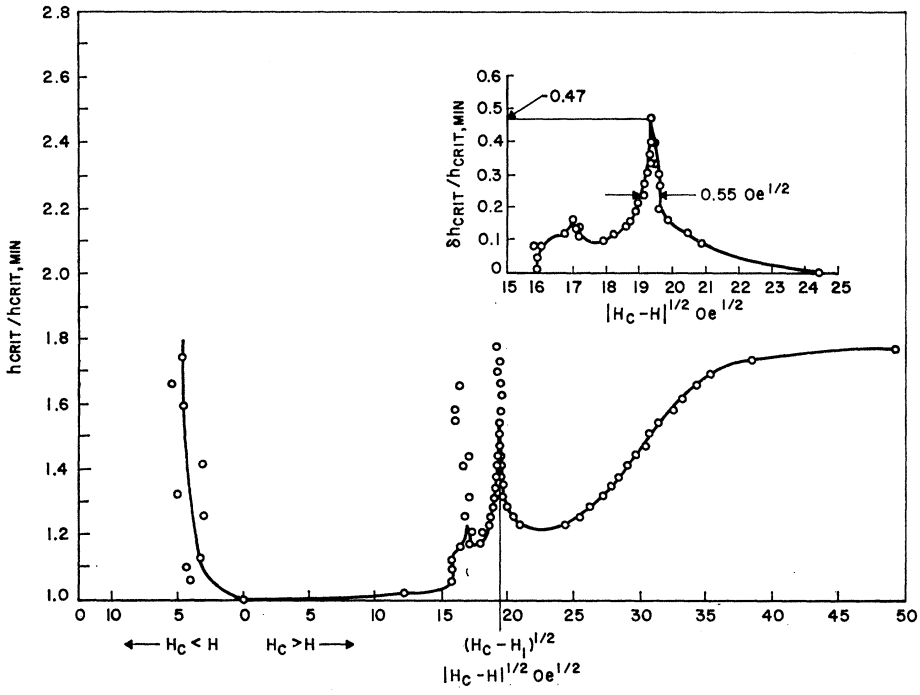

FIG. 4. The parallel-pump threshold curve for EuIG at 20.4°K, with **H** along [111]. The minimum threshold $h_{crit,min}$ is 5.5 Oe.

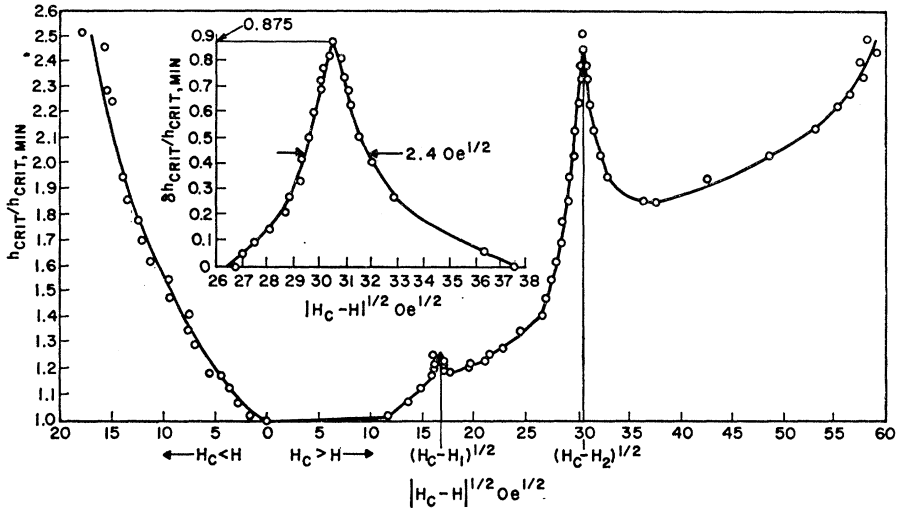

FIG. 5. The parallel-pump threshold curve for EuIG at 4.2°K with **H** along [100]. The $\Delta H_{k\to 0}$ is assumed equal to that found along the [111] direction yielding a minimum threshold $h_{\text{crit, min}}$ of 1.3 Oe.

zation (Figs. 3 and 4), the absence of a shear-wave notch makes the nature of the waves to the right of the longitudinal notch uncertain.

The threshold curves of EuIG parallel pumped along [111] at 4.2 and 20.4°K (Figs. 3 and 4) both appear anomalous for several reasons. Only one notch is found at each temperature whereas two are expected. The exchange constant derived from these notches does not agree with our theoretical estimate (see Appendix A). The shapes of the threshold curves (Figs. 3 and 4) are quite different from those of YIG at the same temperatures (Figs. 1 and 2) and from lithium ferrite at room temperature.[8] The notch at 20.4°K (Fig. 4) has a peculiar shape even though EuIG is elastically quite isotropic (see Table II). These anomalies are undoubtedly connected with the large magnetoelastic coupling constant of EuIG along [111]. For this reason we measured the threshold curve with the magnetic field along [100] where the coupling constant is much smaller[11] and this yielded more consistent results (Fig. 5). The two notches are in the expected relative positions as mentioned above and yield an exchange constant in agreement with the theory given in Appendix A. Also, we can now at least partially interpret the threshold curves (Figs. 3 and 4) taken with the magnetic field along [111]. The notches are probably longitudinal ones which have been shifted to higher k values by the spin-elastic wave interaction. This effect was first predicted by Morgenthaler[6] for the shear-wave notch. The experimentally observed shift is 90 Oe which makes the exchange constant derived from the shifted notch erroneously high. The expression for the shift[6] in our notation is

$$H_s=\frac{2\gamma_{\text{eff}}h_{\text{crit}}Q_e}{\omega_p}\left(\frac{\omega_1{}^0+\omega_m}{\omega_1{}^0}\right)^{1/2}W^2,$$

where W is the width of the notch in units of $(H_c-H)^{1/2}$; $Q_e{}^{-1}$ is the elastic loss factor, and h_{crit} is the threshold rf magnetic field at the notch. The internal magnetic field at the notch is $\omega_1{}^0/\gamma_{\text{eff}}$. Using data discussed below and summarized in Table II, the shift is calculated to be 97 Oe, in good agreement with the experimental value given above. The anomalous shape of the notch at 20.4°K (Fig. 4) makes it difficult to determine a reliable width so that a significant calculation of the shift at this temperature cannot be made. The absence of the

TABLE I. Calculated and experimental magnetic fields for minimum threshold.

	EuIG		YIG	
	4.2°K	20.4°K	4.2°K	20.4°K
Saturation magnetization $4\pi M$ (G)	1320[a]	1320[a]	2470[a]	2470[a]
Anisotropy field H_a along [111] (Oe)	5046[b]	5022[b]	165[d]	165[d]
Gyromagnetic ratio $\gamma_{\text{eff}}/2\pi$ (sec^{-1} Oe$^{-1}\times 10^{-6}$)	1.54[c]	1.54[c]	2.80[d]	2.80[d]
Pump frequency (Gc/sec)	34.72	34.72	34.78	34.70
H_c, applied field at minimum threshold (Oe)				
calculated, [111] direction	6076	6100	5710	5695
experimental, [111] direction	5932	5985	5703	5692
experimental, [100] direction[e]	17 520			

[a] S. Geller, H. J. Williams, R. C. Sherwood, J. P. Remeika, and G. P. Espinosa, Phys. Rev. **131**, 1080 (1963).
[b] W. G. Nilsen (unpublished).
[c] Reference 1.
[d] G. P. Rodrigue, H. Meyer, and R. V. Jones, J. Appl. Phys. **31**, 376S (1960).
[e] Magnetic resonance data on EuIG along [100] at liquid-helium temperatures is not available. The pump frequency in this experiment was 32.94 Gc/sec. From the above data, it is roughly estimated that $K_1/M=-3500$ Oe and $K_2/M=-1100$ Oe for EuIG at 4.2°K.

TABLE II. Elastic and magnetic properties of EuIG and YIG.

	EuIG		YIG	
	4.2°K	20.4°K	4.2°K	20.4°K
Density (gm/cm)[3]	6.31[a]	6.31[a]	5.17[a]	5.17[a]
Elastic constant $c_{11}\times10^{-11}$ (dyn/cm²)	25.2[c]	25.2[c]	26.9[b]	26.9[b]
Elastic constant $c_{44}\times10^{-11}$ (dyn/cm²)	7.60[c]	7.60[c]	7.64[b]	7.64[b]
Elastic constant $c_{12}\times10^{-11}$ (dyn/cm²)	10.70[c]	10.70[c]	10.77[b]	10.77[b]
Elastic anisotropy $2c_{44}/(c_{11}-c_{12})$	1.048[c]	1.048[c]	0.947[b]	0.947[b]
Shear velocity $v_s(100)^{d}\times10^{-5}$ (cm/sec)	3.47[c]	3.47[c]	3.84	3.84
Shear velocity $v_s(110)^{d}\times10^{-5}$ (cm/sec)	3.39[c]	3.39[c]	3.94	3.94
Longitudinal velocity $v_l(110)^{d}\times10^{-5}$ (cm/sec)	6.36[c]	6.36[c]	7.15	7.15
Longitudinal notch $(H_c-H_1)^{1/2}$(Oe)$^{1/2}$	16.75[e]	···	9.15	10.1
Shear notch $(H_c-H_2)^{1/2}$(Oe$^{1/2}$)	30.40[e]	···	19.25	19.1
Ratio $[H_c-H_2/H_c-H_1]^{1/2}$	1.81	···	1.97	1.89
Ratio v_l/v_s	1.83	1.83	1.86	1.86
Exchange constant (shear notch) $D\times10^{9}$ (Oe cm²)	5.3	···	4.6	4.5
Exchange constant (longitudinal notch) $D\times10^{9}$ (Oe cm)	5.6	···	4.2	4.5
Magnetoelastic coupling constant (erg/cm³$\times10^{-6}$)				
parallel pump values $\frac{1}{3}(2B_1+B_2)$	···	···	18	11
parallel pump values $\frac{1}{3}\sqrt{2}(B_1-B_2)$	104	···	15	8.5
strain-gauge values $\frac{1}{3}(2B_1+B_2)$	···	···	4.3[g] (78°K)	4.3[g] (78°K)
strain-gauge values $\frac{1}{3}\sqrt{2}(B_1-B_2)$	96[f] (78°K)		1.8[g] (78°K)	1.8[g] (78°K)
parallel pump B_1	272	···	7.2	5.2
parallel pump B_2	45	···	41	23
strain gauge B_1	227[f] (78°K)	···	2.3[g] (78°K)	2.3[g] (78°K)
strain gauge B_2	22[f] (78°K)	···	8.2[g] (78°K)	8.2[g] (78°K)
Elastic $Q_e\times10^{-4}$ longitudinal notch	4.2	0.5	7.5	1.4
Elastic $Q_e\times10^{-4}$ shear notch[e]	2.8	···	13	2.8

[a] G. P. Espinosa, J. Chem. Phys. **34**, 2344 (1962).
[b] A. E. Clark and R. E. Strakna J. Appl. Phys. **32**, 1172 (1961). We assume that these constants are independent of temperature.
[c] The velocity measurements of EuIG were kindly carried out for us by T. B. Bateman of Bell Telephone Laboratories. The elastic constants were derived from the velocity using standard formulas given, for example, in W. P. Mason, *Physical Acoustics and the Properties of Solids* (D. Van Nostrand Company, Inc., New York, 1958).
[d] Propagation in the (110) direction and particle displacement in the direction indicated.
[e] From the threshold curve taken along the hard [100] axis.
[f] See Ref. 11. The measurements were made at 78°K.
[g] See Ref. 19. The measurements were made at 78°K.

shear-wave notch along [111] is discussed at the end of the next section.

In the region where $H_c<H$, the k values are so small that the plane-wave analysis[2] used in finding Eq. (1) probably is not valid. A combination of Eqs. (1) and (2) does not predict the curves in Figs. 1–5, and the sudden increase in $h_{\rm crit}$ as H is increased above H_c is probably due to surface effects rather than to variation in $\sin^2\theta_k$. The origin of the peculiar shape of the threshold curve at $H>H_c$ for EuIG at 4.2°K (Fig. 3) is not known.

DISCUSSION

Spin-Wave Linewidth

The spin-wave linewidth for minimum threshold ($\Delta H_{k\to0}$) was determined using Eq. (1) and assuming $\theta=\pi/2$. The minimum threshold ($h_{\rm crit,min}$) was found by calibrating the cavity with the YIG sphere for which this quantity was known.[12] For EuIG parallel pumped along [111], $\Delta H_{k\to0}$ was 0.075 and 0.32 Oe at 4.2 and 20.4°K, respectively, compared to 0.015 and 0.062 Oe, respectively, for YIG. We assume that $\Delta H_{k\to0}$ for EuIG pumped along [100] at 4.2°K is the same as along [111], namely, 0.075 Oe. These linewidths are not likely to be the intrinsic values for pure EuIG or YIG at these low temperatures but are more likely determined by small amounts of impurity.

In the region where nearly pure spin waves are excited (usually away from the notches), the threshold curves show the dependence of spin-wave linewidth (ΔH_k) on wave number. Sparks *et al.*[13] have calculated the contribution of the three-magnon confluence process to ΔH_k. They find for $\theta_k=\pi/2$ and assuming $k_BT\gg\frac{1}{2}\omega_p\times[1+\frac{1}{2}\omega_p/4\gamma_{\rm eff}D_{\rm eff}k^2]$ and $\frac{1}{2}\omega_p\gg4\gamma_{\rm eff}D_{\rm eff}k^2$ that

$$\partial\Delta H_k(\text{three-magnon})/\partial k=[\mu_B{}^3k_BT/\hbar^3]\times[4\pi M/\gamma_{\rm eff}{}^2\tfrac{1}{2}\omega_pD_{\rm eff}],$$

where μ_B is the Bohr magneton. The calculated and observed results are given in Table III. For YIG, the

TABLE III. Spin-wave linewidth for YIG and EuIG at 4.2 and 20.4°K along [111].

	EuIG		YIG	
	4.2°K	20.4°K	4.2°K	20.4°K
Linewidth for minimum threshold $\Delta H_{k\to0}$ (Oe)	0.075	0.32	0.015	0.062
$\partial\Delta H_k/\partial k\times10^{9}$ (Oe cm) expt	270 (210)[a]	1300	39	82
$\partial\Delta H_k$ (3-magnon)$/\partial k\times10^{9}$ (Oe cm) calc	14	68	7.1	35

[a] Parallel pumped along [100] (see Fig. 5).

[12] E. G. Spencer, R. C. LeCraw, and R. C. Linares, Jr., Phys. Rev. **123**, 1937 (1961).

[13] M. Sparks, R. Loudon, and C. Kittel, Phys. Rev. **122**, 791 (1961).

spin-wave linewidth is proportional to k as predicted by theory, and the slope of ΔH_k versus k increases with increasing temperature but not at a sufficient rate to be proportional to T. Also, the magnitude of $\partial\Delta H_k/\partial k$ found for YIG is larger than predicted for the three-magnon confluent process, suggesting that other k-dependent processes may be important in determining ΔH_k. For EuIG parallel-pumped along [111], the magnetoelastic interaction obscures much of the pure spin-wave linewidth, and only a crude estimate of $\partial\Delta H_k/\partial k$ can be made. The temperature dependence of $\partial\Delta H_k/\partial k$ is close to that predicted by theory but the magnitude is much too high. This might indicate that the pumped waves are largely elastic rather than magnetic since the absent shear-wave notch should be in this part of the threshold curve. The theory of the three-magnon confluence process also predicts that ΔH_k will fall off from its linear dependence on k when k becomes large enough so that the assumption $\frac{1}{2}\omega_p \gg 4\gamma D k^2$ is no longer valid. Such behavior is observed for EuIG at 20.4°K (see Fig. 4) but not for YIG at either temperature. Much closer agreement between theory and experiment is found at room temperature for both YIG[10] and lithium ferrite.[8]

Exchange Field

The exchange constant for spin-wave dispersion [Eq. (2)] can be evaluated since the wave numbers at the longitudinal and shear notches are known. For YIG at a pump frequency of 34.7 Gc/sec, D is about 4.5×10^{-9} Oe cm^2 at both 4.2 and 20.4°K (see Table II). The shift in shear-wave notch predicted by Morgenthaler[6] should be small and is not included in the determination of D. Using the parallel-pump technique but a lower pump frequency (11.38 Gc/sec), LeCraw and Walker[5] found $D=4.9\times10^{-9}$ Oe cm^2 for YIG at our low temperatures. Also, specific-heat measurements[14,15] yield 4.5×10^{-9} Oe cm^2 for D, in excellent agreement with the parallel-pump measurements. The close agreement between exchange constants determined at two different pump frequencies and from specific-heat measurements is further evidence for the k^2 form of the exchange term in Eq. (2) and gives one some confidence in the parallel-pump method of determining D in cases where the magnetoelastic coupling is small. The parallel-pump measurement of D is reliable to within about 5%.

The exchange constant for YIG can also be found from the molecular-field coefficients (J's) using the relation[16,17]

$$D=\frac{5}{16\gamma\hbar}(5J_{cd}-8J_{aa}-3J_{dd})a^2,$$

where $a=12.38$ Å is the lattice constant. Using the values of J given by Douglass[16] ($J_{ad}=4.8\times10^{-15}$ ergs, $J_{dd}=2.1\times10^{-15}$ ergs, and $J_{aa}=1.1\times10^{-15}$ ergs), we find 2.3×10^{-9} Oe cm^2 for D. This low value of D supports the contention of Smart,[18] in connection with the specific-heat measurements, that the above values of J_{dd} and J_{aa} derived from a molecular-field analysis are too large. A similar discrepancy between calculated and measured values of D exists with lithium ferrite.[8]

The intrinsic exchange constant for EuIG $D=\mu\mathbf{M}_{10}+2\beta\mathbf{M}_{20}$ was found to be 5.5×10^{-9} Oe cm^2, which is slightly larger than the value for YIG. This increase in the value of D is due to the positive value of the term $2\beta\mathbf{M}_{20}$ in Eq. (2). In Appendix A, we estimate using molecular-field theory the ratio $D_{\mathrm{EuIG}}/D_{\mathrm{YIG}}$ to be 1.18, yielding $D_{\mathrm{EuIG}}=5.3\times10^{-9}$ Oe cm^2 in improbably good agreement with the experimental value given above. The ratio of effective exchange constants is 2.23 so that $D_{\mathrm{eff}}=10.0\times10^{-9}$ Oe cm^2.

Magnetoelastic Coupling Constant

Morgenthaler[6] has derived the expression for the width of the shear-wave notch for the dc magnetic field along [100]. In our notation, the width in units of $(H_c-H)^{1/2}$ is given by

$$W=B_2\left[\frac{4\pi\omega_1{}^0\gamma_{\mathrm{eff}}}{2c_{44}\omega_m(2\omega_1{}^0+\omega_m)}\right]^{1/2},$$

where c_{44} is one of the elastic stiffness constants (see Table II) and $\omega_1{}^0/\gamma_{\mathrm{eff}}$ is the internal magnetic field at the spin–elastic-wave crossover. For the magnetic field along [111], Comstock and Nilsen[8] have shown that the effective magnetoelastic coupling constant changes in the above expression from B_2 to $\frac{1}{3}(2B_1+B_2)$. For the longitudinal-wave notch, we show in Appendix B that the effective coupling constant is $\frac{1}{3}\sqrt{2}(B_1-B_2)$ and c_{11} replaces c_{44}. In this section we compare the magnetoelastic coupling constants obtained from parallel-pump measurements with those derived from strain-gauge measurements which have been made on EuIG[11] and YIG[19] down to 78°K.

For YIG, B_1 and B_2 have the same sign[19] and $c_{11}>c_{44}$, so that the above analysis predicts that the longitudinal notch should be narrower than the shear notch. This is found to be the case for YIG at both 4.2 and 20.4°K, as can be seen in Figs. 1 and 2. The effective magnetoelastic coupling constants derived from the width of the two notches are given in Table II. Also, since the effective coupling constants are different for the longitudinal and shear notch, the individual coupling constants B_1 and B_2 can be determined. These are also given in Table II for YIG at 4.2 and 20.4°K together with the strain-gauge measurements at 78°K. Our parallel-pump values are somewhat larger than the coupling constants

[14] S. S. Shinozaki, Phys. Rev. **122**, 388 (1961).
[15] J. E. Kunzler, L. R. Walker, and J. K. Galt, Phys. Rev. **119**, 1609 (1960).
[16] R. L. Douglass, Phys. Rev. **120**, 1612 (1960).
[17] H. Meyer and A. B. Harris, J. Appl. Phys. **31**, 495 (1960).
[18] J. S. Smart, in *Magnetism*, edited by G. T. Rado and H. Suhl (Academic Press Inc., New York, 1963), Vol. III.
[19] S. Iida and R. Blair (to be published).

derived from the strain-gauge measurements,[19] but this difference might reflect higher values of B_1 and B_2 at the lower temperatures at which the parallel-pump experiments were done. Indeed, the measured coupling constants increase with decreasing temperature as expected. At room temperature, the agreement between B_2 derived from parallel-pump and strain-gauge measurements is much better. Courtney and Clarricoats found $B_2=7.32\times10^6$ erg cm^2 at a pump frequency of 9.2 Gc/sec and Olsen found $B_2=4.7\times10^6$ erg cm^3 at 23.2 Gc/sec whereas the strain-gauge measurements[19] yielded $B_2=5.5\times10^6$ erg cm^3.

Both B_1 and B_2 can also be determined for EuIG at 4.2°K since the effective magnetoelastic coupling constant is different for the longitudinal-wave notch with **H** along [111] and the shear-wave notch with **H** along [100]. The values found for B_1 and B_2 are given in Table II together with Iida's strain-gauge measurements[11] made at 78°K. For EuIG, the agreement between parallelpump and strain- gauge measurements is reasonably good. The magnetoelastic coupling constants were not determined for EuIG at 20.4°K since the longitudinal notch with its odd shape is not likely to yield a reliable width and no other notch was found to allow the individual B's to be determined.

Elastic Q

The height of $(\delta h_{\rm crit})_{\rm max}$ of the shear-wave notch is a measure of the elastic losses of the sample at half the pump frequency. The expression for Q_e was first derived by Morgenthaler[6] and in our notation is[20]

$$Q_e=\frac{2(H_e-H_{1,2})}{(\delta h_{\rm crit})_{\rm max}}\left(2\frac{\omega_1{}^0}{\omega_m}+1\right).$$

The measured values of $(\delta h_{\rm crit})_{\rm max}$ are shown in Figs. 1–5, and the calculated values of Q_e are given in Table II. For both EuIG and YIG, the elastic losses are lower at the lower temperature, and EuIG has a lower Q_e than YIG. Olson[7] has measured Q_e for YIG at 78°K by the same technique as used here. He found $Q_e=1.8\times10^4$ at $\omega_p/2=11.6$ Gc/sec. Assuming Q_e^{-1} varies linearly with frequency, a Q_e of 1.2×10^4 is predicted for YIG at $\omega_p/2=17.6$ Gc/sec, in reasonable agreement with our measurements at 20.4°C.

Absence of Shear Notch Along [111] for EuIG

There are three possible reasons why no shear-wave notch is observed for EuIG parallel pumped along [111] at 4.2 and 20.4°K. First, the notch may be shifted to higher k values than can be parallel pumped. Second, the notch may have such a large width as to be unrecognizable. Third, the spin-wave instability may merge smoothly into the elastic-wave instability.[21]

[20] E. W. Courtney and P. J. B. Clarricoats, J. Electron. Control **16**, 1 (1964).
[21] R. L. Comstock, J. Appl. Phys. **35**, 2427 (1964).

Concerning the first possible reason, the shift [Eq. (5)] depends on $h_{\rm crit}$ at the notch (about 1.5 times larger for the shear than the longitudinal notch), Q_e of the notch (about the same for the two notches), and W^2 (the width of the shear notch squared). For $B_1\gg B_2$, W^2 increases by a factor $2c_{11}/c_{44}=6.6$ so that the shift for the shear notch should be about $1.5\times6.6\times90=900$ Oe and the shear notch should be located at about $(H_c-H_2)^{1/2}=[(30.40)^2+900]^{1/2}=43$. This part of the threshold curve was parallel pumped (see Figs. 3 and 4), but no evidence of the shear-wave notch was found. The width of the shear notch should be about $(6.6)^{1/2}=2.6$ times the width of the longitudinal notch, or about 8 Oe$^{1/2}$ at 4.2°K. A notch with this width should easily be observed.

The criteria for the spin-wave instability to merge smoothly into elastic-wave instability is given by Comstock[21] as

$$\omega_m\omega_p c_{44}M_s/2\gamma_{\rm eff}{}^2B_{\rm eff}{}^2Q_e\Delta H_{k_0}<1,$$

where $B_{\rm eff}=\frac{1}{3}(2B_1+B_2)\approx196\times10^6$ erg cm^3 from the data on the other notches in EuIG. The left side of the equality equals 7.4 for the shear notch at 4.2°K, predicting that the shear-wave notch should be normal contrary to observation. This last calculation is the least reliable of the three given above since it depends on the absolute magnitude of the quantities given in the inequality. In contrast, the shift and linewidth are known for the longitudinal notch and only the ratio need be estimated which depends only on c_{11}/c_{44}. Also, the left side of the above inequality tends to be smaller for the two shear-wave notches which are absent and larger for the notches which are observed. Nevertheless, the cause for the absence of the shear-wave notch in EuIG along [111] is not definitely known.

CONCLUSIONS

Both the k-independent and k-dependent parts of the spin-wave linewidth of YIG are less than that of EuIG at low temperatures. Also, the three-magnon confluence process[13] does not account quantitatively for the k-dependent linewidth at low temperatures. The exchange constant for YIG measured by the parallel-pump technique agrees well with specific-heat measurements but is about twice that predicted from molecular-field theory. The exchange constant of EuIG is predicted quite accurately by considering the induced moment of the Eu^{3+} ions and its effect on the spin-wave spectrum of the iron lattice and estimating the relative parameters using molecular-field theory. The large magnetoelastic coupling constant of EuIG parallel pumped along [111] makes the threshold curve quite anomalous. The longitudinal notch is shifted to significantly higher k values yielding an erroneously high exchange constant. Also, the shear-wave notch is absent, possibly because the spin-wave instability merges smoothly into the elastic-wave instability. Along [100], the magnetoelastic

coupling constant of EuIG is much smaller, and a normal threshold curve is observed. The magnetoelastic coupling constants derived from parallel-pump measurements agree well for EuIG and are somewhat higher for YIG than the strain-gauge measurements. The origin of the discrepancy for YIG is not known but it should be noted that the parallel-pump measurements were made at 4.2 and 20.4°K and the strain-gauge measurements were made only down to 78°K. The elastic Q increases with decreasing temperature for both garnets and is larger for YIG than for EuIG, as expected.

ACKNOWLEDGMENTS

The authors are indebted to J. P. Remeika for supplying the crystals and T. B. Bateman for the velocity measurements.

APPENDIX A: CONTRIBUTION OF THE Eu^{3+} IONS TO THE SPIN-WAVE EXCHANGE STIFFNESS OF EuIG

Wolf and Van Vleck[9,22,23] have discussed the magnetic moment and ferromagnetic resonance of EuIG. A straightforward extension of their ideas may be made to the spin-wave spectrum.

The iron sublattices are supposed tightly coupled together to form a single sublattice of magnetization $\mathbf{M}_1$. The energy density of this lattice consists of a magnetic part $-\mathbf{H}_0\cdot\mathbf{M}_1$ in the internal dc magnetic field $\mathbf{H}_0$ and an exchange part, which may be expressed as $-\frac{1}{2}\lambda\mathbf{M}_1\cdot\mathbf{M}_1-\frac{1}{2}\mu\mathbf{M}_1\cdot\nabla^2\mathbf{M}_1$, where λ and μ are positive. The ratio μ/λ, which has the dimensions (length)^2, is proportional to the mean squared displacement between interacting iron ions, these squared displacements being weighted by the strengths of the corresponding exchange interactions.

The Eu^{3+} ion has special properties which allow its effect on the resonance spectrum to be calculated in a simpler way than that of other rare-earth ions. (See, for example, the treatment of Tb impurities in Ref. 24.) One knows that the free ion has a $J=0$ ground state and that as a consequence such properties as a magnetic moment and an anisotropy energy which it possesses in EuIG, must arise from admixtures into the ground state of higher J states. The interaction responsible for this is that of the ion with the dc magnetic field and the exchange field of the iron. Because the energy separation of the excited J manifolds from the $J=0$ state and the crystal field splittings of the excited J states are all large compared to microwave frequencies, the admixture effects are sensibly frequency-independent. The energy arising from the presence of the Eu^{3+} in EuIG may then be taken to be a frequency-independent functional of the internal dc magnetic field and the exchange field of the iron ions. Since the latter is proportional to $\mathbf{M}_1$, the energy of the whole system may be expressed in terms of $\mathbf{M}_1$. In a phenomenological treatment we sum over the inequivalent rare-earth sites, and the energy functional is consistent with the lattice symmetry. We therefore consider the various contributions to the total energy and show that this is now the energy density for a lattice of moment $\mathbf{M}_1$ whose parameters are modified from those of the simple iron lattice.

Wolf and Van Vleck[9] showed that the interaction, $2(\mathbf{H}_{ex}+\mathbf{H}_0)\cdot\mathbf{S}+\mathbf{H}_0\cdot\mathbf{L}$, of the Eu^{3+} ion with the internal dc magnetic field and the exchange field $\mathbf{H}_{ex}=\alpha\mathbf{M}_1$ of the iron-europium interaction, produces a magnetic moment $\mathbf{M}_2$ on the europium proportional to $\mathbf{H}_0+2\alpha\mathbf{M}_1$. We may now write

$$\mathbf{M}_2=\chi(\mathbf{H}_0+2\alpha\mathbf{M}_1),$$

where since χ is supposed frequency-independent the relation holds for time-varying quantities generally. The energy density E_1 associated with this interaction is

$$\begin{aligned}E_1&=-\tfrac{1}{2}\chi(\mathbf{H}_0+2\alpha\mathbf{M}_1)\cdot(\mathbf{H}_0+2\alpha\mathbf{M}_1),\\&=-\tfrac{1}{2}\chi\mathbf{H}_0\cdot\mathbf{H}_0-2\alpha\chi\mathbf{M}_1\cdot\mathbf{H}_0-2\alpha^2\chi\mathbf{M}_1\cdot\mathbf{M}_1.\end{aligned}$$

This term applies to the uniform part of the magnetization. The part E_2 due to nonuniform terms may be written

$$\begin{aligned}E_2&=-\beta/\alpha\cdot\tfrac{1}{2}\chi(\mathbf{H}_0+2\alpha\mathbf{M}_1)\cdot\nabla^2(\mathbf{H}_0+2\alpha\mathbf{M}_1),\\&=-\beta\chi(\mathbf{H}_0+2\alpha\mathbf{M}_1)\cdot\nabla^2\mathbf{M}_1.\end{aligned}$$

β/α, like μ/λ, is connected with the weighted mean-squared separation of interacting iron and europium ions.

The anisotropy energy E_3 is simply an unspecified functional of $\mathbf{M}_1$ having cubic symmetry. It is therefore no different from any familiar anisotropy term. Confining ourselves to easy or hard directions, we may replace it by a fictitious magnetic field $\mathbf{H}_a$ parallel to $\mathbf{H}_0$, which it will be convenient to suppose acts on the total rf moment $\mathbf{m}_1+\mathbf{m}_2$ of the system. Thus,

$$\begin{aligned}E_3&=-\mathbf{H}_a\cdot(\mathbf{m}_1+\mathbf{m}_2)\\&=-\mathbf{H}_a\cdot\mathbf{m}_1(1+2\alpha\chi).\end{aligned}$$

Finally, the rf dipolar energy density E_4 is given by the usual expression, which for a spatial dependence $e^{i\mathbf{k}\cdot\mathbf{r}}$ is just $-[4\pi(\mathbf{k}\cdot\mathbf{m}_1+\mathbf{m}_2)^2]/(\mathbf{k}\cdot\mathbf{k})$. Thus, we have

$$E_4=-[4\pi(\mathbf{k}\cdot\mathbf{m}_1)^2/(\mathbf{k}\cdot\mathbf{k})](1+2\alpha\chi)^2.$$

The total energy of the system is now given by

$$\begin{aligned}E=&-\mathbf{H}_0\cdot\mathbf{M}_1-\tfrac{1}{2}\lambda\mathbf{M}_1\cdot\mathbf{M}_1-\tfrac{1}{2}\mu\mathbf{M}_1\cdot\nabla^2\mathbf{M}_1\\&-\tfrac{1}{2}\chi\mathbf{H}_0\cdot\mathbf{H}_0-2\alpha\chi M_1\cdot\mathbf{H}_0-2\chi\alpha^2\mathbf{M}_1\cdot\mathbf{M}_1\\&-\beta\chi[\mathbf{H}_0+2\alpha\mathbf{M}_1]\cdot\nabla^2\mathbf{M}_1+\{-\mathbf{H}_a\cdot\mathbf{m}_1(1+2\alpha\chi)\\&-4\pi[(\mathbf{m}_1\cdot\mathbf{k})^2/(\mathbf{k}\cdot\mathbf{k})](1+2\alpha\chi)^2\},\end{aligned}$$

where the last two terms are connected with rf energy alone. Introducing the dc moments $\mathbf{M}_{10}$ and $\mathbf{M}_{20}$ of the

[22] W. P. Wolf, J. Phys. Soc. Japan **15**, 2104 (1960).
[23] J. H. Van Vleck, Phys. Rev. **123**, 58 (1961).
[24] J. F. Dillon, Jr., and L. R. Walker, Phys. Rev. **124**, 1401 (1961).

iron and europium sublattices we must have

$$\mathbf{M}_{20}=\chi(\mathbf{H}_0+2\alpha\mathbf{M}_{10}).$$

We have the relation $2\alpha\chi\sim\mathbf{M}_{20}/\mathbf{M}_{10}$, since $2\alpha\mathbf{M}_{10}\gg\mathbf{H}_0$. Clearly $\mathbf{M}_{20}$ and $\mathbf{M}_{10}$ lie in the same line. We continue to write them as vectors to emphasize that they may be (and, in fact, are) antiparallel; that is, $\mathbf{M}_{20}/\mathbf{M}_{10}$ means $(M_{20}/M_{10})\,\mathrm{sgn}\mathbf{M}_{20}\cdot\mathbf{M}_{10}$. Similarly $\mathbf{H}_0$ can be dropped from the coefficient of $\nabla^2\mathbf{M}_1$ and E can finally be taken to be

$$E=-\mathbf{H}_0\cdot\mathbf{M}_1(1+\mathbf{M}_{20}/\mathbf{M}_{10})-(\tfrac{1}{2}\lambda+2\alpha^2\chi)\mathbf{M}_1\cdot\mathbf{M}_1$$
$$-(\tfrac{1}{2}\mu+\beta(\mathbf{M}_{20}/\mathbf{M}_{10})\mathbf{M}_1\cdot\nabla^2\mathbf{M}_1-\tfrac{1}{2}\chi\mathbf{H}_0\cdot\mathbf{H}_0$$
$$-\left\{\mathbf{H}_a\cdot\mathbf{m}_1(1+\mathbf{M}_{20}/\mathbf{M}_{10})-4\pi\frac{(\mathbf{m}_1\cdot\mathbf{k})^2}{\mathbf{k}\cdot\mathbf{k}}(1+\mathbf{M}_{20}/\mathbf{M}_{10})^2\right\}.$$

This is now the energy density for a single lattice in an internal dc magnetic field $\mathbf{H}_0(1+\mathbf{M}_{20}/\mathbf{M}_{10})$ and anisotropy field $\mathbf{H}_a(1+\mathbf{M}_{20}/\mathbf{M}_{10})$; it has a dc exchange constant $\lambda+4\alpha^2\chi$ and a stiffness parameter $\mu+2\beta\mathbf{M}_{20}/\mathbf{M}_{10}$. Formally, the factor $(1+\mathbf{M}_{20}/\mathbf{M}_{10})^2$ in the rf dipolar energy can be considered as modifying $\sin\theta_k$, where θ_k is the angle between the spin-wave propagation and the magnetization, to $(1+\mathbf{M}_{20}/\mathbf{M}_{10})\sin\theta_k$. The lattice still has the gyromagnetic ratio γ_{Fe}, and its spin-wave frequencies will satisfy the usual formula

$$\left(\frac{\omega}{\gamma_{\mathrm{Fe}}}\right)^2=\{(\mathbf{H}_0+\mathbf{H}_a)(1+\mathbf{M}_{20}/\mathbf{M}_{10})$$
$$+\mathbf{M}_{10}(\mu+2\beta(\mathbf{M}_{20}/\mathbf{M}_{10}))(\mathbf{k}\cdot\mathbf{k})\}$$
$$\times\{(\mathbf{H}_0+\mathbf{H}_a)(1+\mathbf{M}_{20}/\mathbf{M}_{10})+\mathbf{M}_{10}(\mu+2\beta(\mathbf{M}_{20}/\mathbf{M}_{10}))$$
$$\times(\mathbf{k}\cdot\mathbf{k})+4\pi\mathbf{M}_{10}\sin^2\theta_k(1+\mathbf{M}_{10}/\mathbf{M}_{20})^2\},$$

or, alternatively,

$$\left\{\frac{\omega}{\gamma_{\mathrm{Fe}}(1+\mathbf{M}_{20}/\mathbf{M}_{10})}\right\}^2=\left\{\mathbf{H}_i+\frac{\mu\mathbf{M}_{10}+2\beta\mathbf{M}_{20}}{1+(\mathbf{M}_{20}/\mathbf{M}_{10})}\mathbf{k}\cdot\mathbf{k}\right\}$$
$$\times\left\{\mathbf{H}_i+\frac{\mu\mathbf{M}_{10}+2\beta\mathbf{M}_{20}}{1+(\mathbf{M}_{20}/\mathbf{M}_{10})}\mathbf{k}\cdot\mathbf{k}+4\pi(\mathbf{M}_{10}+\mathbf{M}_{20})\sin^2\theta_k\right\},$$

where $\mathbf{H}_i=\mathbf{H}_0+\mathbf{H}_a$, in which form the effective gyromagnetic ratio $\gamma_{\mathrm{eff}}=\gamma_{\mathrm{Fe}}(1+\mathbf{M}_{20}/\mathbf{M}_{10})$ for ferromagnetic resonance is more clearly shown. We associate the intrinsic exchange constant D with the quantity

$$D=\mu\mathbf{M}_{10}+2\beta\mathbf{M}_{20},$$

since the term $(1+\mathbf{M}_{20}/\mathbf{M}_{10})$ just changes the effective applied field. The ratio of D for EuIG to that for YIG is thus $1+2\beta\mathbf{M}_{20}/\mu\mathbf{M}_{10}$. To make an estimate of the new D we use some admittedly naive ideas from molecular-field theory. In YIG we know that D is proportional[16] to $5J_{ad}-8J_{aa}-3J_{dd}$, where the J's are molecular-field parameters. The mean square displacements $\langle r_{ad}^2\rangle$, $\langle r_{aa}^2\rangle$, $\langle r_{dd}^2\rangle$ are in the ratio 5:12:6, and it follows that μ/λ is proportional to

$$\frac{5J_{ad}-12(\frac{2}{3}J_{aa})-6(\frac{1}{2}J_{dd})}{J_{ad}-\frac{2}{3}J_{aa}-\frac{1}{2}J_{dd}}=2.94,$$

using the values of J quoted by Douglass.[16] The rare-earth–ion interaction is thought to be primarily with the tetrahedral ions. There are 6 such tetrahedral neighbors, 4 with mean square distance 6 and 2 with the value 4 in the units used above. This gives β/α proportional to 5.33. The value αM_{10} is given by Wolf and Van Vleck as 24°K. From molecular-field theory $\lambda M_{10}=(3/S+1)\times(1/g)T_C=234$°K. M_{20}/M_{10} is 0.47. Combining these values we have

$$D_{\mathrm{EuIG}}/D_{\mathrm{YIG}}=[1+2\times0.47\times5.33/2.94\times24°/234°]$$
$$=1.18.$$

The experimental value is 1.21. The excellent agreement must be considered to be largely fortuitous since one's faith in the values of the J's is very limited. In particular the ratio of J_{aa}, J_{dd} to J_{ad} is probably considerably overestimated in the molecular-field theory. A decrease in this ratio would raise the number 2.94 and thus lower the predicted value of $D_{\mathrm{EuIG}}/D_{\mathrm{YIG}}$. However, it is reassuring to find that the sign and magnitude of the change in D are correctly estimated.

APPENDIX B: MAGNETOELASTIC COUPLING TO LONGITUDINAL ELASTIC WAVES

The magnetoelastic energy for the case of static magnetization along the [111] axis in a cubic ferromagnet is given in Ref. 8. The equations of motion for this case are derived for longitudinal waves in the present appendix. The relevant energy is[8]

$$U_{me}=\sqrt{2}/3(B_1-B_2)[\alpha_x\alpha_z(e_{xx}-e_{yy})], \qquad \text{(B1)}$$

where $\boldsymbol{\alpha}=\mathbf{M}/M$ and e_{ij} is the ij component of the strain. The equations of motion follow from $d\boldsymbol{\alpha}/dt=(\gamma/M)\boldsymbol{\alpha}\times\nabla_\alpha U_{me}$ and $\rho\ddot{R}_x=\partial^2U_{me}/\partial x\partial e_{xx}+\partial^2U_{me}/\partial y\partial e_{xy}+\partial^2U_{me}/\partial x\partial e_{xz}$, resulting in the following equations of motion for $\partial/\partial y=\partial/\partial z=0$:

$$\dot{M}_x=-(\omega_H+\omega_s\cos\omega_p t)M_y,$$
$$\dot{M}_y=(\omega_H+\omega_m+\omega_s\cos\omega_p t)M_x+\gamma B_{\mathrm{eff}}\partial R_x/\partial x, \qquad \text{(B2)}$$
$$\rho\ddot{R}_x=c_{11}\partial^2R_x/\partial x^2+(B_{\mathrm{eff}}/M)\partial M_x/\partial x,$$

where $B_{\mathrm{eff}}=(\sqrt{2}/3)(B_1-B_2)$. The volume dipolar field, parallel-pumping field, dc field, and elastic restoring force are included as in the case of shear waves.[6,21] The above equations are the same as those for shear waves given in Ref. 21 except B_{eff} replaces B_2 and c_{11} replaces c_{44}. All of the previous analysis for the determination of coupling constants, elastic Q, and field shift done for the shear waves can therefore be carried over to longitudinal waves with the above replacements.